



# Investigation of the effect of cutting tool edge radius on material separation due to ductile fracture in machining

Yiğit Karpat\*

Bilkent University, Department of Industrial Engineering, Ankara 06800, Turkey

## ARTICLE INFO

### Article history:

Received 3 November 2008

Received in revised form

19 May 2009

Accepted 25 May 2009

Available online 3 June 2009

### Keywords:

Micromachining

Ductile fracture

Cutting tool edge radius

## ABSTRACT

This paper investigates the interaction between cutting tool edge radius and material separation due to ductile fracture based on Atkins' model of machining. Atkins' machining model considers the energy needed for material separation in addition to energies required for shearing at the primary shear zone and friction at the secondary shear zone. However, the effect of cutting tool edge radius, which becomes significant at microcutting conditions, was omitted. In this study, the effect of cutting tool edge radius is included in the model and its influence on material separation is investigated. A modification to the solution methodology of Atkins' machining model is proposed and it is shown that the shear yield stress and the fracture toughness of the work material can be calculated as a function of uncut chip thickness.

© 2009 Elsevier Ltd. All rights reserved.

## 1. Introduction

In machining, the energy required for the formation of new surfaces was calculated to be negligible compared to shearing and friction in early studies [1]. Recently, Atkins [2] pointed out the fact that a separation criterion is employed in finite element simulations of metal cutting operations in order to simulate the movement of the cutting tool into the workpiece, whereas no such mechanism is used for finite element analysis of metal forming. In analytical machining models, even though the energy required for the separation of work material and chip is recognized [1], it is usually neglected when compared to shearing and friction energies. After making this observation, Atkins proposed a metal cutting model where ductile fracture mechanics is used to explain the chip formation mechanism. Atkins modified Merchant's [3] orthogonal machining model by considering the fracture toughness of the workpiece material as the specific work of surface formation and calculated the surface creation energy to be in the range of  $\text{kJ}/\text{m}^2$ . Atkins concluded that the energy spent on ductile fracture is not negligible and becomes comparable to energy spent on friction at small uncut chip thickness; therefore it can be used to explain and model size effect in machining. Astakhov [4] also stated that machining is different from other metal-forming operations and fracture initiates chip formation thus generating new surfaces. Subbiah and Melkote [5] evaluated the Atkins model and presented experimental evidence of ductile material separation that supports the findings of Atkins. They took

photographs of the chip roots during the machining of oxygen-free-high-conductivity copper (OFHC) and aluminum alloy (AL 2024-T3) by employing a quick stop mechanism and identified the fracture zones. They also considered the effect of the edge radius and showed that tensile stresses exist in front of the round-edged cutting tools, creating favorable conditions for fracture to occur by using finite element analysis [6]. Rosa et al. [7] employed finite element simulations of machining and the effect of fracture was included as a correction term to increase the accuracy of cutting force predictions. Wyeth [8] extended the Atkins model such that the fracture modes at different cutting conditions were identified. It was shown that the fracture mode and toughness change with the rake angle.

Size effect is the non-linear abrupt increase of specific cutting energy at micromachining conditions. This phenomenon has been observed when machining many different materials under various cutting conditions and plays an important role in better understanding and modeling tool-based micromachining [9]. In literature, there are several explanations that relate size effect to the material strengthening mechanisms due to (i) the decreasing number of defects in microstructure [10], (ii) the increasing strain rate at the primary shear zone [11], (iii) the decreasing effect of thermal softening [12], and (iv) the effect of strain gradient plasticity at the deformation zones [13] at low uncut chip thickness. The effects of material strengthening mechanisms can be modeled by using material constitutive models [14]. In addition to these, cutting tool edge radius [15] is also considered to explain size effect in machining. The effect of cutting tool edge radius has been studied by using analytical and computational techniques. It has been shown that the tool edge radius influences the chip formation mechanism, and a tertiary shear zone at the

\* Tel.: +90 3122902264; fax: +90 3122664054.

E-mail address: [ykarpat@bilkent.edu.tr](mailto:ykarpat@bilkent.edu.tr)

### Nomenclature

$F_c$	cutting force
$F_p$	ploughing force
$F_r$	frictional rake face force
$m$	friction factor
$r$	cutting tool edge radius
$R$	fracture toughness
$t_e$	effective uncut chip thickness
$t_u$	uncut chip thickness
$V$	cutting speed
$w$	width of cut

$Z$	dimensionless parameter
$\alpha$	rake angle
$\alpha_e$	effective rake angle
$\beta$	friction angle
$\beta_r$	friction angle at the tool–chip interface
$\beta_p$	friction angle at the tool–work interface
$\phi$	shear angle
$\gamma$	primary shear zone shear strain
$\lambda$	inclination angle of the stagnant metal zone
$\rho$	prow angle
$\tau_y$	shear yield stress
$\zeta_1$	slip-line angle

tool–workpiece interface is believed to be responsible for additional cutting forces. The studies on the influence of edge radius on chip formation and cutting forces were pioneered by Albrecht [16] by modifying the Merchant model to include the effects of ploughing. Hsu [17] and Abdelmoneim and Scrutton [18] used extrapolation techniques on the cutting force data and studied the effect of cutting tool edge radius. Manjunathaiah and Endres [19] developed a model based on the work of Connolly and Rubenstein [20] to determine cutting and ploughing forces as a function of tool edge radius. Waldorf et al. [21] considered two different approaches, i.e. stagnation point and stable built-up zone, in his slip-line model and found results favoring the formation of a stable built-up zone in front of the tool. Karpát and Özel [22] investigated the relation between the inclination angle of the stable built-up zone and the frictional conditions and found that inclination angle decreases as friction increases. Woon et al. [23] studied the contact phenomenon on the cutting edge by using small field of view photography method and identified the sticking and sliding zones on the cutting tool by using finite element analysis. It is found that the stagnation point on the cutting edge remains stationary at all experimental uncut chip thickness values ranging from 2 to 20  $\mu\text{m}$ . However, it is also possible to consider this zone as a stable built-up edge (dead metal zone) by investigating the velocity profiles given in the study, which are obtained from finite element simulations.

Understanding the mechanics of tool-based micromachining such as the effect of tool edge radius, material strengthening mechanisms, and ductile fracture mechanics is important in order to select and optimize cutting conditions. The material separation due to ductile fracture mechanics and its relationship with the cutting tool edge radius during machining have not been studied in detail. This study aims to investigate this interaction by using analytical methods and experimental cutting data. In this study, the Atkins machining model is extended to include the effect of edge radius, and a modified solution methodology that allows the calculation process outputs such as shear yield stress, friction angle, and fracture toughness is presented.

## 2. The Atkins machining model

Atkins [2] considered the basic machining model proposed by Merchant [3] and integrated the work of surface creation in addition to plasticity and friction work. He concluded that the reason why Merchant's metal cutting theory cannot yield good results is not related to the complexity of the model, but instead to its non-material dependency. With the addition of the fracture toughness (specific work of surface formation) term in the Merchant model, Atkins was able to obtain results that are in good agreement with experimental observations. With the proposed algorithm, the shear yield stress and fracture toughness

of a work material can be calculated. According to this model, the cutting power during orthogonal machining considering shearing, friction, and fracture (Fig. 1) can be written as

$$F_c V = \frac{\tau_y t_u V w \cos \alpha}{\sin \phi \cos(\phi - \alpha)} + \frac{F_c \sin \beta \sec(\beta - \alpha) V \sin \phi}{\cos(\phi - \alpha)} + R w V \quad (1)$$

where  $\tau_y$  is the shear yield stress,  $t_u$  is the uncut chip thickness,  $V$  is the cutting speed,  $\alpha$  is the rake angle,  $\phi$  is the shear angle,  $w$  is the width of cut,  $F_c$  is the cutting force,  $\beta$  is the friction angle, and  $R$  is the fracture toughness. The first term on the right-hand side of this equation is related to the plastic work on the primary shear zone, the second term is related to the frictional work at the secondary shear zone, and the last term is related to the surface work in front of the cutting tool. This model assumes cutting tool to be sharp; therefore no work for ploughing was considered.

The minimum energy principle ( $\partial F_c / \partial \phi = 0$ ) can be applied to Eq. (1) and Eq. (2) is obtained. Eq. (2) can be used to calculate shear angle for a given cutting condition if the friction angle and the ratio of fracture toughness to shear yield stress are known. In Eq. (2), the dimensionless parameter denoted by  $Z$  ( $Z = R/\tau_y t_u$ ) introduces material property in minimum energy expression:

$$\left[ 1 - \frac{\sin(\beta) \sin(\phi)}{\cos(\beta - \alpha) \cos(\phi - \alpha)} \right] \left[ \frac{1}{\cos^2(\phi - \alpha)} - \frac{1}{\sin^2(\phi)} \right] = -[\cot(\phi) + \tan(\phi - \alpha) + Z] \times \left[ \frac{\sin(\beta)}{\cos(\beta - \alpha)} \left( \frac{\cos(\phi)}{\cos(\phi - \alpha)} + \frac{\sin(\phi) \sin(\phi - \alpha)}{\cos^2(\phi - \alpha)} \right) \right] \quad (2)$$

The relationship between the cutting force and the uncut chip thickness in terms of material properties can be obtained if Eq. (1) is rewritten in the form of a line equation as

$$F_c = \left( \frac{\tau_y w \gamma}{Q} \right) t_u + \frac{R w}{Q} \quad Q = [1 - (\sin(\beta) \sin(\phi) / \cos(\beta - \alpha) \cos(\phi - \alpha))] \quad (3)$$

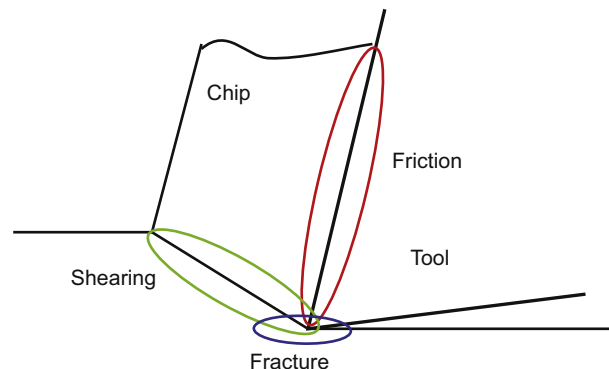


Fig. 1. Distribution of energies spent in machining.

where the slope and the intercept of the line equation are defined according to shear yield stress, fracture toughness, shear angle, rake angle and friction angle. Primary shear zone shear strain is denoted by  $\gamma$ . In Atkins' solution methodology, cutting and thrust force data are utilized to calculate friction angle  $\beta$  and the shear angle  $\phi$  is obtained from Eq. (2) for various values of  $Z$ . Fracture toughness and shear yield stress are calculated through an iterative methodology that makes use of experimental slope and intercept values. Therefore, by using a constant fracture toughness to shear yield stress ratio, cutting forces at any uncut chip thickness can be calculated. The term  $Q$  includes the combined effect of rake angle, friction angle, and shear angle. As uncut chip thickness approaches zero, the value of  $Q$  approaches unity, therefore affecting the slope and intercept values of the cutting force curve. In machining studies, it has been shown that the effect of cutting tool edge radius becomes significant as uncut chip thickness decreases. The effect of edge radius is implemented in the Atkins methodology in the next section.

### 3. Including the effect of edge radius in Atkins' machining model

Karpat and Özel [22] investigated the influence of curvilinear cutting tool edges on the mechanics of orthogonal cutting during high-speed machining. In their study, a stagnant metal zone in front of the cutting edge was considered, and the effect of the inclination angle ( $\lambda$ ) of the stagnant metal zone on the frictional conditions at the tool–chip and tool–workpiece interfaces was examined through a slip-line field analysis. The slip-line field model used in their study and its hodograph are shown in Fig. 2(a) and (b).

In this model, the front boundary of the stagnant metal zone is assumed to be extending from the rake face for simplicity. Assuming that the chip will be in contact with the rake face of the cutting tool at all cutting conditions, similar to Eq. (1) the following equation can be written:

$$F_c V = \frac{\tau_y t_u V w \cos(\alpha)}{\sin(\phi) \cos(\phi - \alpha)} + \frac{F_r V \sin(\phi)}{\cos(\phi - \alpha)} + \frac{F_p V \sin(\zeta_1 - \lambda)}{\sin(\zeta_1)} + R w V \quad (4)$$

where  $F_r$  is the frictional rake face force and  $F_p$  is the ploughing force as shown in Fig. 2(c). In Eq. (4),  $\zeta_1$  is the slip-line angle, which is dependent on the friction factor ( $m$ ) at the tool–workpiece interface ( $AB$ ) and can be determined according to slip-line field theory as

$$\zeta_1 = 0.5 \cos^{-1}(m) \quad (5)$$

The friction factor,  $m$ , is the ratio of the shear stress at the related region to the shear yield stress at the primary shear zone. The total cutting force can be written by considering the tangential and normal forces acting on the rake face and the underside of the stagnant metal zone:

$$F_c = F_r \frac{\cos(\beta_r - \alpha)}{\sin(\beta_r)} + F_p \frac{\sin(\beta_p + \lambda)}{\sin(\beta_p)} \quad (6)$$

$$F_p = m \tau_y |AB| w \quad (7)$$

In Eq. (6),  $\beta_r$  and  $\beta_p$  represent the friction angles at the tool–chip and tool–work interfaces. The relationship between the friction angle ( $\beta_p$ ) and slip-line angle ( $\zeta_1$ ) at the stagnant metal zone can be written by using slip-line field analysis as in Eq. (7). Prow angle ( $\rho$ ) can be calculated from the hodograph of the slip-line field by considering the velocity continuity:

$$\beta_p = \tan^{-1} \left( \frac{\cos(2\zeta_1)}{1 + \pi/2 - 2\rho + 2\zeta_1 - 2\lambda + \sin(2\zeta_1)} \right)$$

$$\rho = \sin^{-1} \left( \frac{\sin(\lambda)}{\sqrt{2} \sin(\zeta_1)} \right) \quad (7)$$

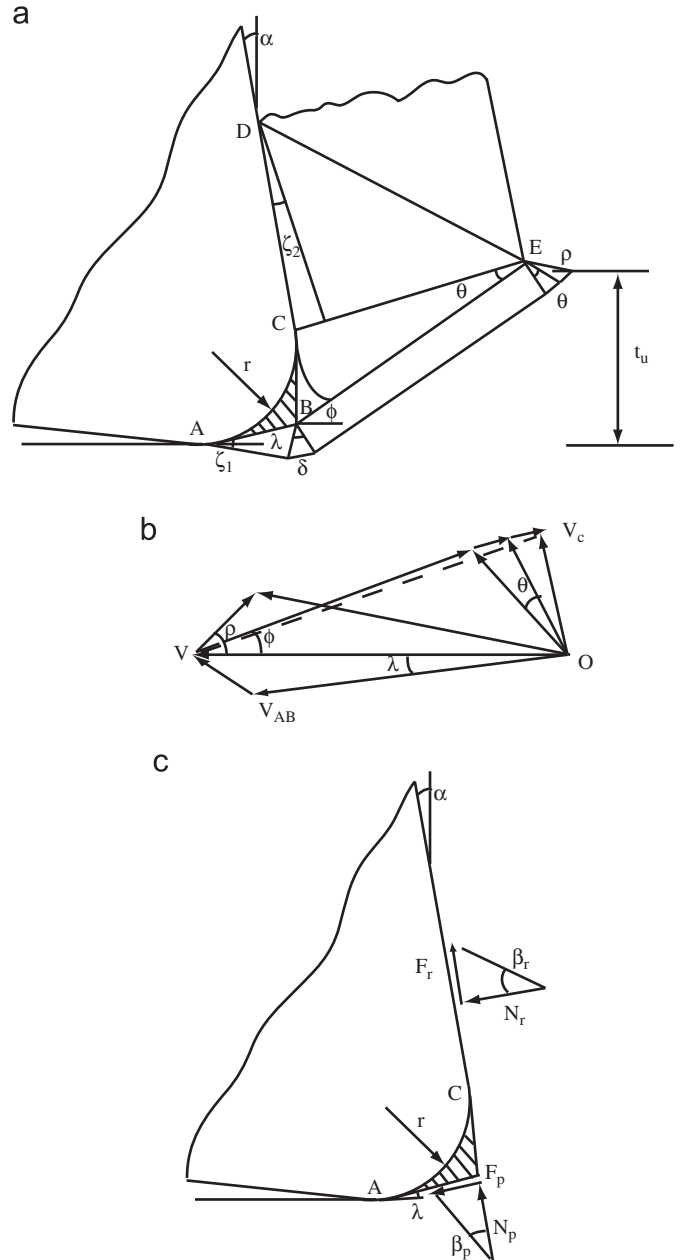


Fig. 2. (a) The slip-line field model for cutting tools with edge radius [22], (b) the hodograph of the slip-line field, (c) the normal and tangential forces acting on the cutting tool.

If Eqs. (5)–(7) are inserted in Eq. (4), the combined effect of the edge radius and the ductile fracture on the cutting force can be obtained:

$$F_c = \left( \frac{\tau_y w \cos \alpha}{\sin(\phi) \cos(\phi - \alpha) Q} \right) t_u + \frac{m \tau_y |AB| w}{Q} \times \left[ \frac{\sin(\zeta_1 - \lambda)}{\sin(\zeta_1)} - \frac{\sin(\beta_p + \lambda) \sin(\beta_r) \sin(\phi)}{\sin(\beta_p) \cos(\beta_r - \alpha) \cos(\phi - \alpha)} \right] + \frac{R w}{Q} \quad (8)$$

$$|AB| = \frac{r(1 + \sin \alpha)}{\cos(\lambda - \alpha)}$$

In this expression, the friction factor at the tool–work interface ( $m$ ), the inclination angle of the stagnant metal zone ( $\lambda$ ), the friction angle at the tool–chip interface ( $\beta_r$ ), the shear flow stress ( $\tau_y$ ), the fracture toughness ( $R$ ) and the shear angle ( $\phi$ ) are the unknowns. The length of the stagnant metal zone ( $AB$ ) is

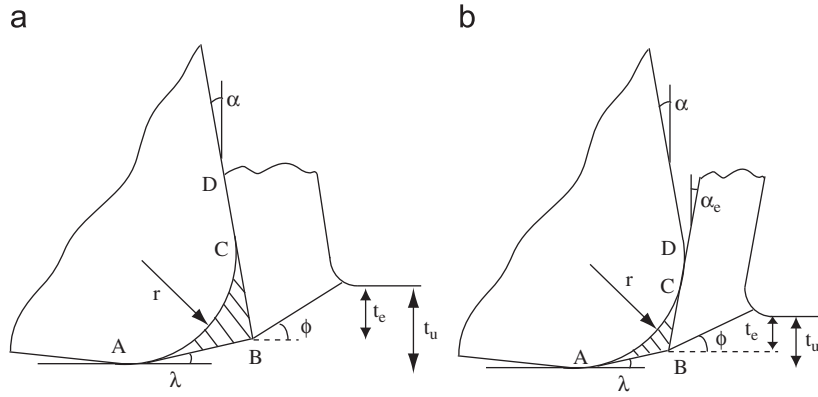


Fig. 3. (a) The relationship between inclination angle and effective uncut chip thickness and (b) the effective rake angle.

dependent on the cutting tool edge radius and the inclination angle. The minimum energy expression in Eq. (2) is not valid for this case. Therefore, derivative of Eq. (8) with respect to shear angle is recalculated as follows:

$$\frac{\sin(\beta_r)}{\cos(\beta_r - \alpha)} \left[ \frac{\cos(\alpha)}{\sin(\phi) \cos(\phi - \alpha)} + \frac{mr(1 + \sin(\alpha))}{t_u \cos(\lambda - \alpha)} \right] \times \left( \frac{\sin(\zeta_1 - \lambda)}{\sin(\zeta_1)} - \frac{\sin(\beta_p + \lambda) \sin(\beta_r) \sin(\phi)}{\sin(\beta_p) \cos(\beta_r - \alpha) \cos(\phi - \alpha)} \right) + Z \quad (9)$$

$$= \left( 1 - \frac{\sin(\beta_r) \sin(\phi)}{\cos(\beta_r - \alpha) \cos(\phi - \alpha)} \right) \times \left[ \frac{\cos(2\phi - \alpha)}{\sin^2(\phi)} + \frac{mr(1 + \sin(\alpha)) \sin(\beta_p + \lambda) \sin(\beta_r)}{t_u \cos(\lambda - \alpha) \sin(\beta_p) \cos(\beta_r - \alpha)} \right]$$

Eq. (8) can be simplified, if sticking contact condition ( $m \cong 1$  and  $\lambda = 0^\circ$ ) at the tool–work interface is assumed. As a result, Eq. (10) can be deduced. The shear strain formulation at the primary shear zone is valid as long as inclination angle is zero or very small:

$$F_c = \left( \frac{\tau_y w \cos \alpha}{\sin \phi \cos(\phi - \alpha) Q} \right) t_u + \frac{Rw}{Q} + \frac{\tau_y r w (1 + \sin(\alpha))}{\cos(\alpha)} \quad (10)$$

When the inclination angle is not assumed to be zero, the effective uncut chip thickness,  $t_e$ , can be calculated depending on the inclination angle as shown in Eq. (11). Depending on the uncut chip thickness value, the chip may be in contact with the rake face of the tool or with the edge radius curvature of the cutting tool. In the latter case, effective rake angle,  $\alpha_e$ , must be considered and can be calculated as in Eq. (12). These two conditions are illustrated in Fig. (3):

$$t_e = t_u - AB \sin(\lambda) \quad (11)$$

$$\alpha_e = a \sin\left(\frac{r - t_e}{r}\right) \quad (12)$$

#### 4. Analysis of the experimental data

The data sets (Table 1, Figs. 4 and 5) reported in [12,24] and Woon et al. [23] are used in this study to calculate process outputs and investigate the effect of edge radius on material separation. The data sets encompass a wide range of uncut chip thickness values ranging from 6 to 200  $\mu\text{m}$  and from 2 to 20  $\mu\text{m}$ . Cutting tools with positive and negative rake angles were employed. The work material is AISI 1045 steel in both of the studies.

Fig. 4 shows the experimental cutting forces obtained from [12]. The experimental slope and intercept values which are required in the Atkins methodology can be calculated from this

Table 1  
Experimental cutting conditions.

	Kopalinsky and Oxley [12]	Woon et al. [23]
Cutting speed (m/min)	420	100
Rake angle (deg)	–5	10
Width of cut (mm)	2	0.3
Uncut chip thickness (mm)	0.006–0.2	0.002–0.02
Work material	AISI 1045	AISI 1045
Edge radius ( $\mu\text{m}$ )	5	10
Cutting tool material	Ceramic	WC-Co

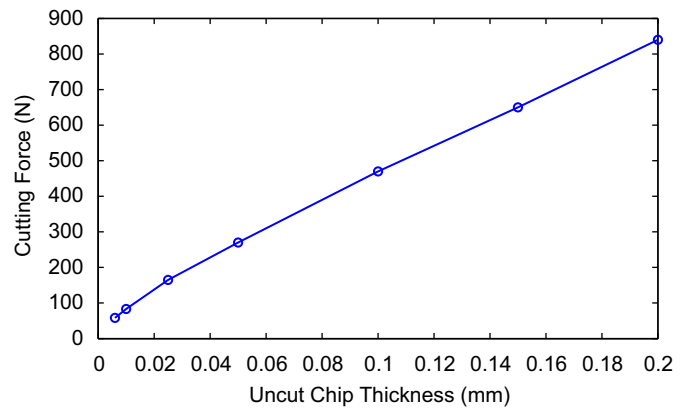


Fig. 4. Experimental cutting force data [12].

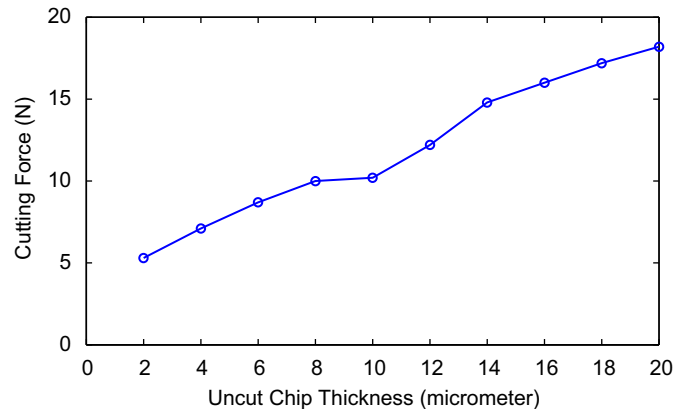


Fig. 5. Experimental cutting force data [23].

figure. In his study, Atkins [2] used two different friction angles (29° and 40°) since no thrust force data were available in [12] and various  $R/\tau_y$  ratios to show that the proposed methodology is able to capture the general trend of the shear angle and size effect. The average shear yield stress was calculated as 391 MPa, which is lower than the experimentally calculated values of 620–980 MPa increasing from the largest uncut chip thickness to the smallest by Kopalinsky and Oxley [12]. According to Atkins, those high shear flow stress values obtained experimentally by Kopalinsky and Oxley [12] occur as a result of neglecting the effect of ductile fracture.

In Fig. 4, the slope of the cutting force curve increases as the uncut chip thickness approaches zero. The effect of tool edge radius becomes significant around 50 μm as the cutting force curve deviates from the constant slope line obtained at large uncut chip thicknesses 0.1–0.2 mm.

In this study, a different solution approach to the Atkins [2] methodology is used to calculate process outputs. Instead of assuming constant slope and an intercept value, varying slope and intercept values are calculated at each uncut chip thickness value, allowing the calculation of shear yield stress, and fracture toughness as a function of uncut chip thickness. The incrementally calculated slope and the intercept values are shown in Table 2. In the first case study, it is assumed that the inclination angle ( $\lambda$ ) is equal to zero. Experimentally measured shear angle values [2,12] are used to calculate the friction angle by using Eq. (2) or (9). The fracture toughness and the shear yield stress values were calculated with and without considering the effect of edge radius. The results are listed in Table 3.

By using the modified solution methodology, it is shown that the shear yield strength increases with decreasing uncut chip thickness due to decreasing shear angle and increasing shear strain at the cutting zone. The fracture toughness decreases as uncut chip thickness decreases and the friction angle increases as uncut chip thickness decreases. With this approach, an exact match between experimental data (cutting force) and model outputs is obtained without assuming constant friction angle and constant  $R/\tau_y$  ratio as in the Atkins [2] methodology. The fracture toughness decreases when edge radius is included in the analysis. It implies that the edge radius creates favorable conditions for the chip–workpiece separation, which is in accordance with the findings of Connolly and Rubenstein [20] and Subbiah and Melkote [6]. Fig. 6 illustrates the variation of fracture toughness

with uncut chip thickness. The fracture toughness, calculated without considering the edge radius, must be equal to zero if cutting force has to intersect the origin at zero uncut chip thickness. However, when the edge radius is considered, this intersection is expected to be on the x-axis. This information can be used to calculate minimum uncut chip thickness in tool-based micromachining. The fracture toughness information has been used to calculate the transition between cutting and rubbing [25] and ductile to brittle transition in micromachining of silicon [26]. However, further experimental research is required on that subject. It must be noted that the slope and the intercept calculations are very sensitive to force measurements.

Table 4 shows the proportions of the total work due to plasticity, friction, and fracture during machining for the experimental data. The proportion of the fracture increases as uncut chip thickness decreases. The proportion of friction remains the same and the proportion of plasticity decreases with decreasing uncut chip thickness. These results reveal the importance of fracture at microscale machining conditions and its influence on the size effect.

The experimental data given in Woon et al. [23] is considered as the second case study where the effect of edge radius and small inclination angle are investigated. The cutting forces obtained by using an ultraprecision turning device are given in Fig. 5. Incremental slopes and intercept points calculated from this curve for two cutting conditions are shown in Table 5.

Table 5 illustrates the process outputs for the experimental data set given in [23]. The cut chip thickness values given in Woon et al. [23] are used to calculate shear angles for corresponding inclination angles. In Woon et al. [23], the physical contact of the chip and the rake face of the cutting tool is captured by using a photographic technique. The rake face contact exists for the cutting conditions from 4 to 20 μm; therefore the situation in Fig. 3(a) is valid for this range.

The fracture toughness and shear yield stress values are found to be in the same order of magnitude for both experimental data

**Table 2**  
Measured values of shear angle and calculated slope and intercept values [12].

Uncut chip thickness (mm)	Shear angle (deg)	Slope	Intercept
0.14	22.5	3700	98.3
0.1	21.9	3800	83.3
0.05	20	4060	70
0.025	18	4560	45.7
0.01	15	5755	26

**Table 3**  
Process outputs calculated from the experimental data ( $\lambda = 0, m = 1$ ).

Uncut chip thickness	Without edge radius effect				With edge radius effect			
	$\beta_r$	$\tau_y$	R	Z	$\beta_r$	$\tau_y$	R	Z
0.14	37.1	409	32.6	0.57	32.48	406	31.2	0.55
0.1	38	410	28	0.65	33.35	408	26.11	0.64
0.05	40	419	23	1.15	35.74	409	21.8	1.07
0.025	43.68	423	15	1.4	39.4	416	13.5	1.3
0.01	48	464	8.3	1.8	45	436	6.5	1.5

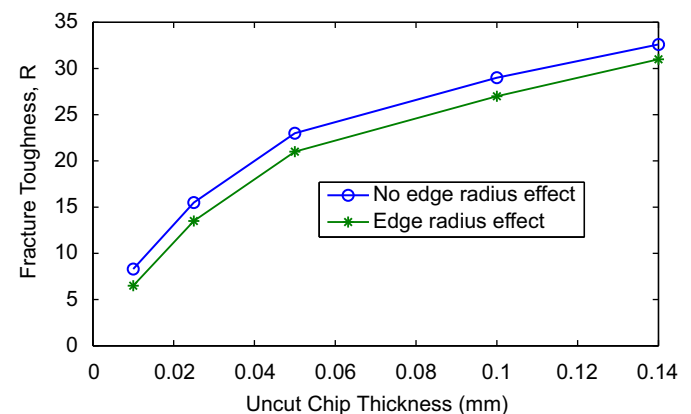


**Fig. 6.** The variation of fracture toughness with uncut chip thickness.

**Table 4**  
The proportions of total work due to plasticity, friction, and fracture.

Uncut chip thickness (mm)	Plasticity (%)	Friction (%)	Fracture (%)
0.14	54.4	35	10.6
0.1	52.8	35.1	12.1
0.05	49.5	33.6	16.9
0.025	46.3	34.9	18.8
0.01	46	34	20

**Table 5**Process outputs calculated from the experimental data [23] ( $m = 0.85$ ).

Uncut chip thickness (mm)	Stagnant metal zone angle (deg)	Slope, intercept	Shear angle (deg)	Friction angle (deg)	Shear yield stress (MPa)	Fracture toughness (kJ/m <sup>2</sup> )	Z
0.016	9	650, 5.5	23.49	50	522	12	1.5
	8		24.06	48.27	525	11	1.2
	5		25.21	44.32	570	10	1.09
0.006	5	750, 4	17.47	57.6	465	7.5	2.68
	3		18.9	54.8	510	6.5	2.1
	2		20	52.1	535	6	1.86
	1		20.8	51	550	5	1.5

sets. Increasing stagnant metal zone inclination angle results in lower shear yield stress and higher fracture toughness values. It must be noted that the actual shear strain may be higher due to non-zero inclination angle which may decrease shear yield stress and increase fracture toughness in order to satisfy experimental slope and intercept values. The shear yield stress is expected to increase as uncut chip thickness decreases due to decreasing shear angle. Therefore, it can be concluded that the inclination angle tends to increase with increasing uncut chip thickness in order to satisfy the continuity of the shear yield stress values.

The shear yield strength values can be employed to calculate material constitutive model parameters. Fracture toughness models can be developed as a function of machining conditions. Thus, the effect of fracture can be integrated in predictive machining models in order to calculate macro/micromachining forces and to model size effect in machining.

## 5. Conclusions

In this study, the influence of the cutting tool edge radius on the material separation via ductile fracture mechanism during machining is studied by using experimental data available in literature. The effect of cutting tool edge radius is integrated into the Atkins machining model. It has been shown that the fracture toughness decreases when the edge radius is considered and the proportion of the fracture work increases with decreasing uncut chip thickness. The fracture toughness is calculated as a function of uncut chip thickness, which may be utilized to estimate the minimum uncut chip thickness for a given a cutting condition. The findings of this study can be used in developing micromachining models, which may be used in selecting machining conditions and designing microcutting tools.

## Acknowledgement

The author would like to thank Prof. M. Rahman for providing part of the orthogonal cutting force data used in this study.

## References

- [1] Shaw MC. Metal cutting principles. 3rd ed. Cambridge, MA: MIT Press; 1954.
- [2] Atkins AG. Modelling metal cutting using modern ductile fracture mechanics: quantitative explanations for some longstanding problems. *Int J Mech Sci* 2003;45:373–96.
- [3] Merchant ME. Mechanics of the metal cutting process. I. Orthogonal cutting and a Type 2 chip. *J Appl Phys* 1945;16(5):267–75.
- [4] Astakhov VP. Metal cutting mechanics. Boca Raton, FL: CRC Press; 1999.
- [5] Subbiah S, Melkote SN. Evaluation of Atkins' model of ductile machining including the material separation component. *J Mater Process Tech* 2007;182:398–404.
- [6] Subbiah S, Melkote SN. Effect of finite edge radius on ductile fracture ahead of the cutting tool edge in micro cutting of AL2024-T3. *Mater Sci Eng* 2008;474:283–300.
- [7] Rosa PAR, Martins PAF, Atkins AG. Revisiting the fundamentals of metal cutting by means of finite elements and ductile fracture mechanics. *Int J Mach Tools Manuf* 2007;47:607–17.
- [8] Wyeth DJ. An investigation into the mechanics of cutting using data from orthogonally cutting Nylon 66. *Int J Mach Tools Manuf* 2008;48:896–904.
- [9] Dornfeld D, Min S, Takeuchi Y. Recent advances in mechanical micromachining. *Ann CIRP* 2006;55(2):745–68.
- [10] Backer WR, Marshall ER, Shaw MC. The size effect in metal cutting. *Trans ASME* 1952;74:61–72.
- [11] Larsen-Basse J, Oxley PLB. Effect of strain-rate sensitivity on scale phenomenon in chip formation. In: Proceedings of the 13th international machine tool design & research conference, University of Birmingham, 1973. p. 209–16.
- [12] Kopalinsky EM, Oxley PLB. Size effects in metal removal process. In: Institute of physics conference series no. 70, third conf mech prop high rates of strain, 1984. p. 389–96.
- [13] Joshi SS, Melkote SN. An explanation for the size-effect in machining using strain gradient plasticity. *Trans ASME J Manuf Sci Eng* 2004;126(4):679–84.
- [14] Johnson GR, Cook WH. A constitutive model and data for metals subjected to large strain, high strain rates and high temperatures. In: Proceedings of seventh international symposium on ballistics, 1983. p. 541–7.
- [15] Komanduri R, Chandrasekaran N, Raff LM. Effect of tool geometry in nanometric cutting: a molecular dynamics simulation approach. *Wear* 1998;219:84–97.
- [16] Albrecht P. New developments in the theory of the metal-cutting process. Part I. The ploughing process in metal cutting. *Trans ASME* 1960;348–358.
- [17] Hsu TC. A study of the shear and normal stresses on a cutting tool. *ASME J Eng Ind* 1966;88:51–64.
- [18] Abdelmoneim M, Scrutton RF. Tool edge roundness and stable build-up formation in finish machining. *ASME J Eng Ind* 1974;96(4):1258–67.
- [19] Manjunathaiah J, Endres WJ. A new model and analysis of orthogonal machining with an edge-radiused tool. *ASME J Manuf Sci Eng* 2000;122:384–90.
- [20] Connolly R, Rubenstein C. The mechanics of continuous chip formation in orthogonal cutting. *Int J Mach Tool Des Res* 1968;8:159–87.
- [21] Waldorf DJ, DeVor RE, Kapoor SG. A slip-line field for ploughing during orthogonal cutting. *ASME J Manuf Sci Eng* 1998;120:693–9.
- [22] Karpat Y, Özel T. Mechanics of high speed cutting with curvilinear edge tools. *Int J Mach Tools Manuf* 2008;48:195–208.
- [23] Woon KS, Rahman M, Neo KS, Liu K. The effect of tool edge radius on the contact phenomenon of tool-based micromachining. *Int J Mach Tools Manuf* 2008;48:1395–407.
- [24] Arsecularatne JA. On tool–chip interface stress distributions ploughing force and size effect in machining. *Int J Mach Tools Manuf* 1997;37(7):885–99.
- [25] Atkins AG, Liu JH. Toughness and the transition between cutting and rubbing in abrasive contacts. *Wear* 2007;262:146–59.
- [26] Venkatchalam S. Predictive modeling for ductile machining of brittle materials. Ph.D dissertation, Georgia Institute of Technology, 2007.